Gerda

Progress Report to the LNGS Scientific Committee

LNGS-EXP 33/05 add. 3/06

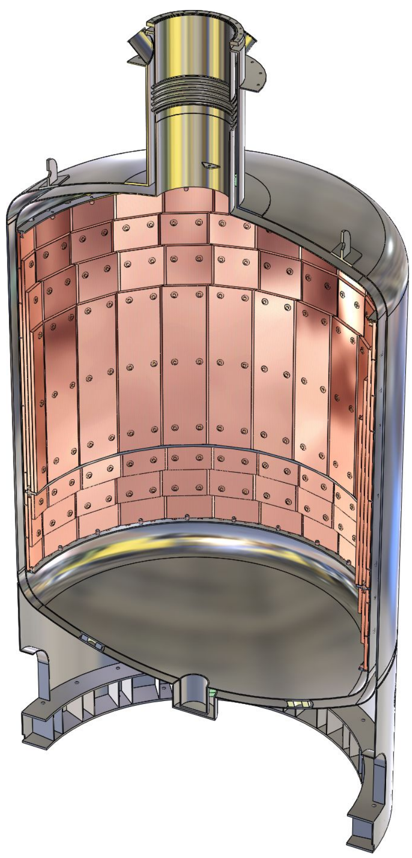

October 2006

I. Abt [j], M. Altmann† [j], A.M. Bakalyarov [i], M. Balata [a], I. Barabanov [g], C. Bauer [c], E. Bellotti [f], S. Belogurov [g,h], S. T. Belyaev [i], M. Bernabe-Heider [c], A. Bettini [k], L. Bezrukov [g], V. Brudanin [b], D. Budjas [c], A. Caldwell [j], C. Cattadori [a,f], O. Chkvorets [c], E. V. Demidova [h], A. Di Vacri [a], M. Di Marco* [c], J. Eberth [d], V. Egorov [b], A. Gangapshev [g], J. Gasparro [m], P. Grabmayr [l], G. Y. Grigoriev [i], K. N. Gusev [i], V. Gurentsov [g], W. Hampel [c], M. Heisel [c], G. Heusser [c], W. Hofmann [c], M. Hult [m], L.V. Inzhechik [i], M. Jelen [j], J. Jochum [l], M. Junker [a], S. Katulina [b], J. Kiko [c], I.V. Kirpichnikov [h], A. Klimenko [b,g], M. Knapp [l], K.T. Knoepfle [c], O. Kochetov [b], V.N. Kornoukhov [g,h], K. Kroeninger [j], V. Kusminov [g], M. Laubenstein [a,f], V.I. Lebedev [i], M. Lindner [c], X. Liu [j], J. Liu [j], B. Majorovits [j], G. Marissens [m], I. Nemchenok [b], L. Niedermeier [l], J. Oehm [c], L. Pandola [a], P. Peiffer [c], A. Pullia [f], F. Ritter [l], C. Rossi Alvarez [k], V. Sandukovsky [b], S. Schoenert [c], J. Schreiner [c], U. Schwan [c], B. Schwingenheuer [c], M. Shirchenko [i], H. Simgen [c], N. Smale [c], A. Smolnikov [b,g], F. Stelzer [j], A.V. Tikhomirov [i], C. Tomei [a], U. Trunk [c], C.A. Ur [k], A.A. Vasenko [h], S.Vasiliev [b,g], D. Weisshaar [d], M. Wojcik [e], E. Yanovich [g], J. Yurkowski [b], S.V. Zhukov [i], E. Zocca [f], G. Zuzel[c]

[a] INFN Laboratori Nazionali del Gran Sasso, Assergi, Italy
[b] Joint Institute for Nuclear Research, Dubna, Russia
[c] Max-Planck-Institut für Kernphysik, Heidelberg, Germany
[d] Institut für Kernphysik, Universität Köln, Germany
[e] Jagiellonian University, Cracow, Poland
[f] Università di Milano Bicocca e INFN Milano, Milano, Italy
[g] Institute for Nuclear Research of the Russian Academy of Sciences, Moscow, Russia
[h] Institute for Theoretical and Experimental Physics, Moscow, Russia
[i] Russian Research Center Kurchatov Institute, Moscow, Russia
[j] Max-Planck-Institut für Physik, München, Germany
[k] Dipartimento di Fisica dell'Università di Padova e INFN Padova, Padova, Italy
[l] Physikalisches Institut, Universität Tübingen, Germany
[m] Institute for Reference Materials and Measurements, Geel, Belgium
†: deceased 31.7.2006
*: on leave from Queens University, Kingston, Canada; now University of Geneva, Switzerland.

Spokesperson: S. Schönert,
(Stefan.Schoenert@mpi-hd.mpg.de)
Co-Spokesperson: C. Cattadori
(Carla.Cattadori@lngs.infn.it)
Technical Coordinator: K.T. Knöpfle
(Karl-Tasso.Knoepfle@mpi-hd.mpg.de)

URL: http://www.mpi-hd.mpg.de/GERDA/gerda-lngs-sc-oct06.pdf

Contents

1 Executive Summary

This report summarizes the accomplished progress of the Gerda collaboration since the last meeting of the Lngs Scientific Committee in March 2006. Relevant issues and recent achievements are highlighted below:

- **Cryostat:** As a consequence of the cost increase of the copper cryostat project by a factor of three with respect to the initial estimate by the same company, the collaboration decided on May 29 to go ahead with the fall back solution, a double-walled super-insulated stainless steel cryostat with internal copper shield. For appropriate background performance, the stainless steel cryostat requires the use of liquid argon (LAr) as shielding and cryogenic liquid. The tender process for the stainless steel cryostat has been closed by September.

- **Safety review:** LNGS has requested for the new cryostat system another safety review which has started with a meeting at Assergi in June. A risk analysis is performed by NIER, Bologna. A preliminary version of the analysis was discussed at CERN on September 18 and 19 with LNGS engineers and external safety consultants. The design of the Gerda experiment and of the new stainless steel cryostat is accepted by the LNGS and its safety advisor, and the final LNGS safety report is expected to be completed at the time of the LNGS SC meeting.

- **Germanium detectors:** The first two enriched crystals for Phase I have been reprocessed successfully at the detector manufacturer. The overall exposure to cosmic ray was less than four days, thus the built-up of cosmogenic isotopes has been kept at an negligible level. 37.5 kg of enriched germanium for Phase II detectors has been transported to Germany is now stored underground to avoid cosmogenic activation. The response and suppression factors of an 18-fold segmented n-type prototype (natural-)germanium detector for Phase II have been analyzed. R&D on background suppression using liquid argon scintillation light is further being pursued.

- **Front-end and DAQ electronics:** Two fully integrated ASIC CMOS chips have been produced and are undergoing currently testing. A system of 24 channels of 14-bit 100 MHz FADC will be ready at the end of this year. Data analysis tools and on-line software for Phase I is available. 240 FADC channels have been procured for the readout of the segmented detectors of Phase II.

- **Water tank and main Gerda building:** The contract for the water tank has been assigned and start of construction is scheduled. The Gerda building design, inclusive platform is completed and the tender will be opened in November.

- **Clean room and lock:** The clean-room is ready for tendering. Solutions for all technical issues regarding the lock are available. The rail system which guides the strings is currently prototyped.

- **Monte Carlo simulations:** The MaGe MC Geant4 framework, developed in close cooperation with the Majorana collaboration, has been extensively used to study muon induced events for the modified detector geometry with stainless steel, copper liner and argon. Moreover, it has been used to study background reduction by detector segmentation as well as liquid argon scintillation. Validation MC simulations by comparison of experimental data with MC has been pursued.

- **Material Screening:** After the decision to construct the GERDA cryostat from stainless steel, special attention has been paid to γ-ray assay of stainless steel samples. Meanwhile, several plates which will actually be used for the cryostat construction have been measured. All samples are within, or even superior to the specifications.

- **Schedule:** A time schedule for the installations in hall A has been worked out. It is based on the input provided by the contracted or bidding companies, and on the resources available at the GERDA institutions. According to this analysis, the infrastructure will be ready for commissioning the germanium detectors in summer 2008.

2 Phase I Detectors

Preparation of the former HdM and Igex detectors for Phase I of Gerda is organized in work packages as introduced in earlier reports. The infrastructures of the underground detector laboratory (LArGe-Facility) which is used for preparing and testing Phase I detectors have been further improved (WP1). New installations in the entrance area have improved the cleanliness level of the clean room. The laboratory is operated as a class 10000 clean room and dedicated areas for detector handling in clean benches have particle densities corresponding to class 10. One clean bench is hermetically closed and flushed with gaseous nitrogen to minimize radon exposure during mounting and testing of enriched detectors. Low-temperature storage for dismounted crystals has been installed. After experiencing high relative humidity during the summer months, the laboratory air is now controlled to about 35% relative humidity. Radon levels in the laboratory are continuously monitored with typical values between 30 and 50 mBq/m^3 of air. WP2 which concerns the testing of the HdM and IGEX detectors prior to dismounting from their cryostat has been completed as described already in the last report. The major activities during the last six months were related to the testing of Phase I prototype detector assemblies (WP3) in liquid argon, the preparation of the integration with cold front-end electronics and DAQ, as well as the dismounting and reprocessing of two enriched diodes (WP4), namely ANG1 and RG3. Moreover, the R&D for the novel background suppression method using liquid argon scintillation light read out at MPIK has been further pursued.

2.1 Operation of prototype detectors in liquid argon

With the decision to adapt the cryostat fall back solution as new baseline design (i.e. stainless steel cryostat with copper lining and liquid argon filling), all subsequent detector tests were carried out in liquid argon. More than 10 warming up and cooling down cycles have been performed with the prototype crystal in argon since then. Tests concerned the optimization of signal and HV contacts, cabling to reduce microphonic noise, mechanical and electrical tests of the low-mass holder, as well as preparation of the integration of crystal and cold front-end electronics. During the last couple cycles, the diode exhibited an increased leakage current, most likely caused by the high humidity during this period. The crystal has been reprocessed at the manufacturer and returned back in operation at LNGS five days later exhibiting normal leakage currents. It is operating stable again since the end of August.

2.2 Transformation of enriched detectors

The HdM and IGEX germanium diodes were produced by different manufactures using distinct techniques. Following our tests with non-enriched prototype crystals, we decided to transform all enriched diodes to one standard technology which is available at an European detector manufacturer. The decision was driven by design simplicity, reliable performance

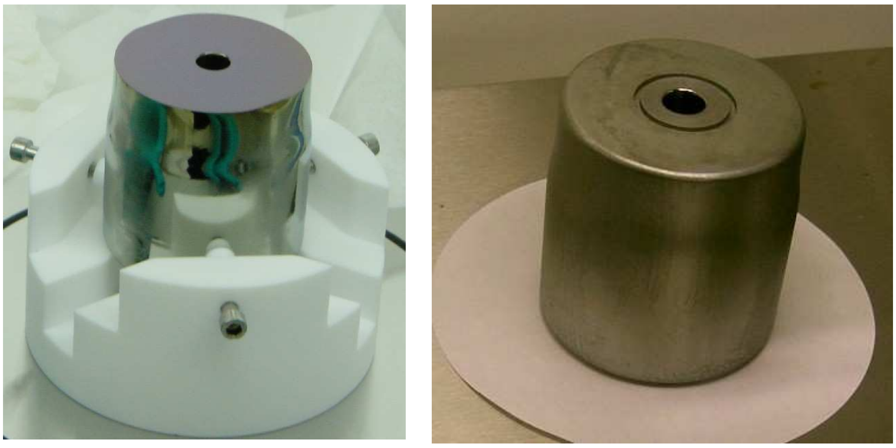

Figure 1: Left: Enriched germanium crystal RG3 (formerly used in the IGEX experiment) after dismounting from its cryostat in the underground detector laboratory at LNGS (LARGE-FACILITY). Right: RG3 during processing.

and logistics. The manufacturer is in the close vicinity of the HADES underground laboratory which is used to store the crystals underground.

In a first step, two enriched diodes, ANG1 and RG3, were removed from their cryostat to verify their dimensions, and prepared for transportation. Following a measurement of the leakage current (I/V curve) in liquid argon of ANG1, both diodes were shipped by car August 21 to the HADES facility for intermediate underground storage. Reprocessing of ANG1 started subsequently at the manufacturer (mechanical modification of the hole, new implantation of the inner contact, new passivation layer and testing). The diode returned underground at Gran Sasso August 26. The overall time of exposure above ground to cosmic rays was 99 hours including transportation. RG3 has been reprocessed in September and is currently stored underground pending shipment to LNGS. The overall time of exposure of RG3 will be approximately 70 hours. The logistic support and underground facilities provided by by IRMM Geel, together with the close cooperation with the manufacturer makes it possible to keep the built up of cosmogenic isotopes at an negligible level during reprocessing. Fig. 1 displays RG3 prior and during reprocessing. The overall loss of enriched material was 20 out of 2121 grams. RG3 and ANG1 will be operated and tested in Phase I detector assemblies in liquid argon in November.

As next major step, it is planned to process the remaining six enriched diodes in one batch, if possible before the end of this year. Moreover, the six non-enriched crystals which have been used in the GENIUS-TF will be refurbished according to the same technique and will be available for GERDA.

2.3 Background suppression by liquid argon scintillation

R&D of the novel background suppression method using the scintillation light of liquid argon (LArGe) has been further pursued at MPIK. This technique is an option considered to be implemented in Gerda in a later phase. The setup (LArGe at MPIK) consists of a 0.39 kg germanium diode submerged in a liquid argon dewar of 20 liter active volume. An 8” PMT views the liquid argon volume which is enclosed with a wavelength shifting reflector. Gamma sources can be inserted up to 8 cm from the crystal. Scintillation light and charge signal are read-out and stored for off-line analysis.

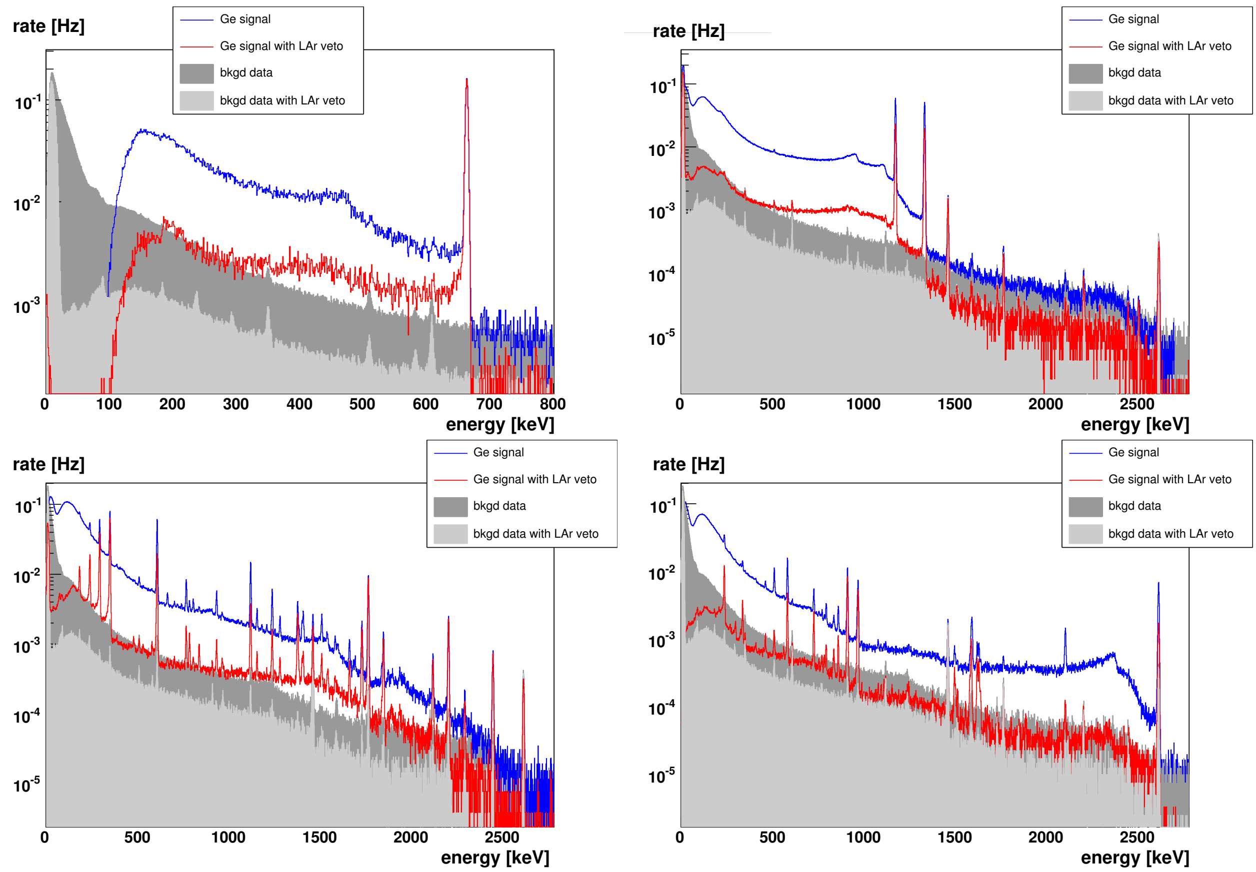

Figure 2: Response to various γ sources placed 8 cm above the crystal inside the liquid argon (LAr). Blue (red) lines correspond to the energy spectra without (with) LAr scintillation suppression. Dark (light) gray spectra show the background of the setup without (with) LAr suppression. Top left: ^{137}Cs (single γ decay); top right: ^{60}Co (decay with two cascading γ's); bottom left: ^{226}Ra (γ cascade); bottom right: ^{232}Th (γ cascade). The obtained suppression factors are limited by the size of the LAr volume.

A yield of 407 ± 10 photo electrons per MeV deposited γ energy has been achieved in these measurements. In the off-line analysis, germanium signals can be vetoed in case of a simultaneous signal detection in the liquid argon. An analysis threshold at the single photo electron level has been applied. Fig. 2 displays the spectrum with and without anti-coincidence for ^{137}Cs, ^{60}Co, ^{226}Ra and ^{232}Th gamma sources. Decays with a single gamma emission as e.g. the ^{137}Cs full energy peak are not suppressed by the argon veto signal while the Compton continuum and gammas emitted in cascades are suppressed. Similar, $0\nu\beta\beta$ events would not be suppressed, while background events at $Q_{\beta\beta}$ typically deposit energy in the liquid argon and can be suppressed.

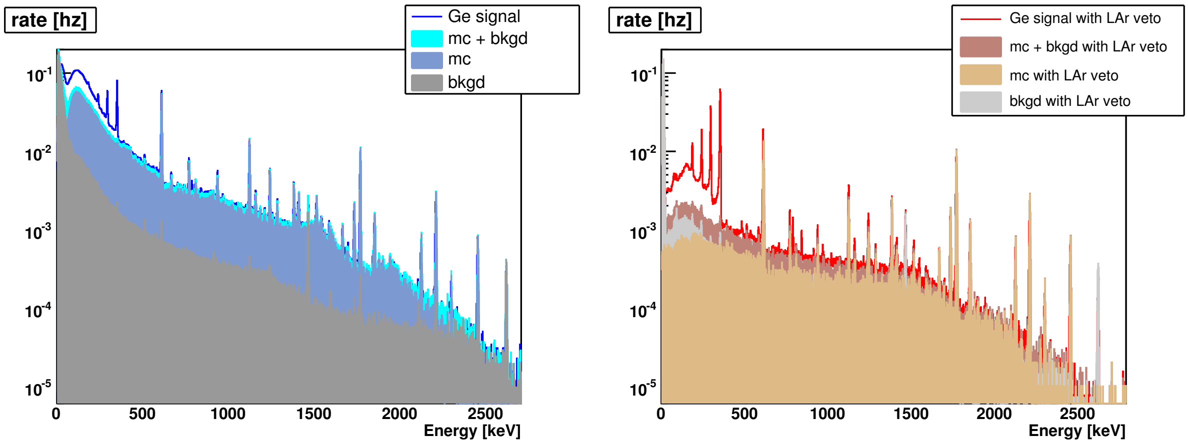

Figure 3: ^{226}Ra gamma spectrum without (left) and with (right) liquid argon suppression in comparison with MaGe MC simulations. Not all progenies have been included in the simulation, thus the missing lines in the MC spectrum at lower energies.

The measured energy spectra have been compared to Monte Carlo simulations using the MaGe package. Fig. 3 displays as an example the ^{226}Ra spectra in comparison with simulation. Good quantitative agreement in the continuum and in the line intensities has been achieved, both with and without argon suppression. The observed suppression factors are depending on the particular radio isotope and on the energy region under consideration. In this setup suppression factors are limited mainly by the small size of the active argon volume (diameter 20 cm height, 40 cm). From MC modeling of an active argon volume of 1 m^3 (or larger), suppression factors of > 100 at $Q_{\beta\beta} = 2.039$ MeV are predicted for ^{60}Co or ^{228}Th sources located close by or internal to the crystal. Such suppression factors will be studied experimentally in the near future in an ultra-low background environment, the LArGe setup at LNGS. The system is currently under construction. It consists of a 90 cm diameter and 200 cm height low background cryostat enclosed in a massive shield. It will become operational in 2007.

Other recent work concerns the increase of the photo electron yield. About 1100 pe/MeV have been achieved without deteriorating the reflectivity of ~ 98 % at 420 nm. The system has now been operated with stable light yield since more than six months. Other work under progress concerns the identification of α, β, γ interactions, as well as neutron backgrounds using the characteristic pulse shape of the argon scintillation light.

3 Phase II Detectors

The enrichment of 37.5 kg of germanium was completed in September 2005. Measurements on samples yielded an isotopic percentage of ^{76}Ge above 87 % and a purity of 99.95 %. This purity is not sufficient for crystal pulling. Several experiments were undertaken at the Germaniy plant in Krasnoyarsk, Russia, to understand the yield of purification to the 99.9999 % level based on $GeCl_4$ chemistry. The best yields were about 75 %. In addition, isotopic dilution was observed after the purification. Given these results, it was decided to transport the unpurified enriched germanium (in the form of GeO_2) to Germany in a transport container specially designed to reduce cosmogenic activation. It arrived in Munich in April 2006 , see fig. 4.

Figure 4: The GeO_2 arrived in Munich in a special transport container. It was weighed and is now stored underground.

The material was then transferred to an underground storage site until further processing steps are defined. The original planning which foresaw new detectors by the end of 2006 will not be met, primarily because of the difficulty in finding a firm to handle the crystal growing with enriched Ge. We are currently investigating different options for crystal pulling, and are in contact with several firms. The purification requirements will depend on the final crystal pulling technology chosen. We now anticipate that two to three years will be needed to produce the Phase II detectors.

The development of “true-coaxial” 18–fold segmented detectors, 6–fold in ϕ and 3–fold in height, is ongoing. A 6–fold–ϕ segmented p-type and an 18–fold segmented n-type detector are available. As the n-type technologoy yields more regular electrical fields, it is preferrable with respect to possible pulse-shape analysis.

The n-type 1.6 kg 18–fold segmented prototype from Canberra–France was intensively tested in a test-setup at the MPI Munich (see fig. 5 top left). Segmented germanium detectors can be used to identify events with photons by using coincidences between the segments of the detectors.

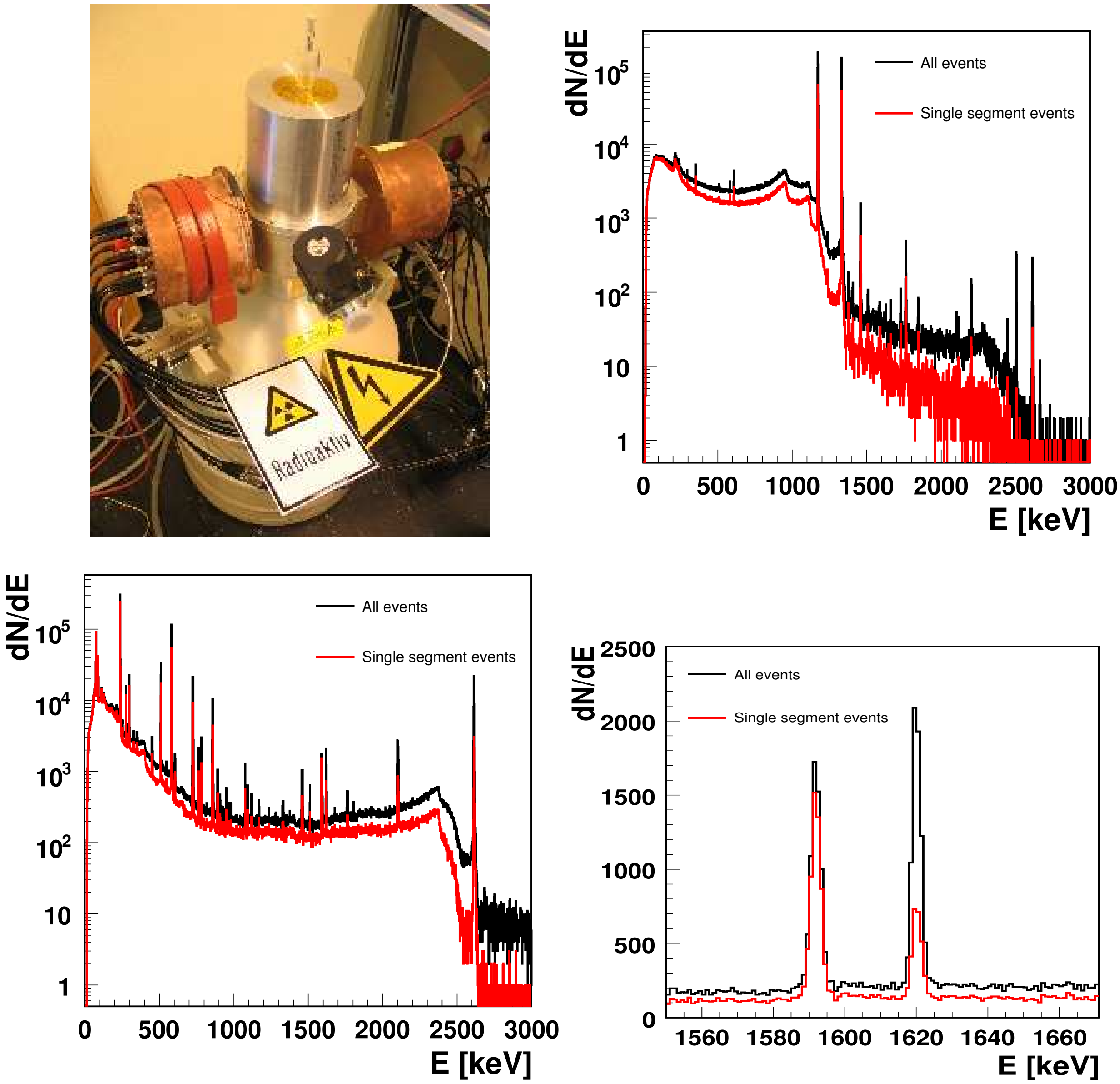

Figure 5: Test-setup with the 18–fold segmented n-type prototype germanium detector. The pre-amplifiers are loacted in two “ears” next to the cryostat [top, left]. Energy spectra of the core electrode for a ^{60}Co source [top, right] and a ^{228}Th source [bottom]. The black line always represents all events, the red line represents events with only one segment hit. The threshold for each electrode was set to 15 keV. After background subtraction the suppression of events in the $Q_{\beta\beta}$-region was measured to be > 90 for the ^{60}Co source and approximately 2 for the ^{228}Th source. The bottom right graph shows that the double escape peak from the 2.6 MeV ^{208}Tl line is not suppressed while the 1.6 MeV ^{212}Bi line is suppressed by a factor of approximately 3. Events in the former line deposit energy on a millimeter-scale while photons in the latter line scatter with a range of the order of centimeters.

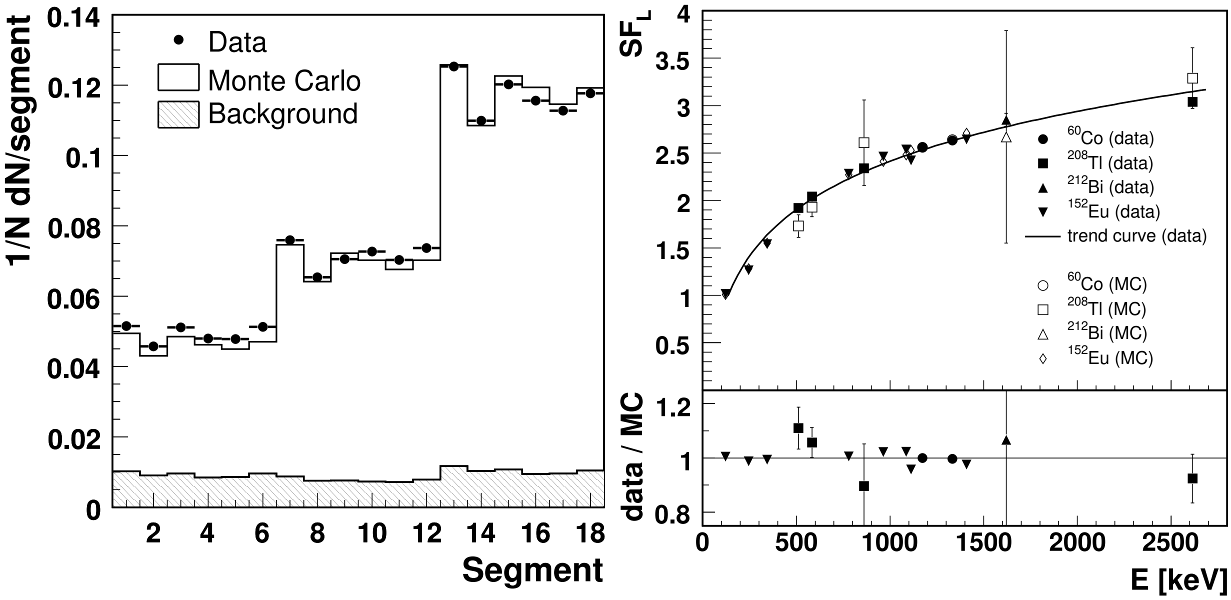

Figure 6: Left: The response of the 18 segments to a ^{60}Co source placed 10 cm above the detector. The background which is always subtracted is also shown. Right: The suppression factor is given for data and Monte Carlo for various energies.

The data obtained with the prototype detector were analyzed in detail with respect to photon identification. After ambient background subtraction the suppression of events in the $Q_{\beta\beta}$-region was measured to vary between 2 and 100, depending on the source and geometry. For gamma emitters placed at a macroscopic distance the suppression varies between 1 and 3 depending on the energy. Fig. 5 shows the spectra obtained for ^{60}Co and ^{228}Th sources placed 10 cm above the center of the detector and the suppression achieved by selecting single segment events. In case of the two–gamma–emitter ^{60}Co placed inside the detector volume a supression factor above 100 can be achieved.

The data was also used to verify the MaGe Monte Carlo program. The teststand and the detector were modeled and the predictions compared with data. For all comparisons data were used where the source was placed 10 cm above the center of the detector. Fig. 6 left shows the number of hits in the 18 segments. Segments 1 to 6 are at the bottom of the crystal, 7 to 12 in the center and 13 to 18 at the top. The higher multiplicity at the top results from self-shielding which the Monte Carlo describes well. The modulation in each group is due to the non-radial drifts which are caused by the crystal axis. This effect is stronger in one hemisphere than in the other which can be modeled by assuming different impurities. The right plot in fig. 6 compares the suppression factors predicted by MC and observed for different gamma energies. The agreement between data and Monte Carlo is extremely good. The absolute values of the factors are of minor importance as they are geometry dependent.

The developement of the copper suspension system is well advanced. Prototypes are available. Stress tests for complete strings composed of 5 detectors were passed successfully with a saftey factor of three. The tooling needed to mount crystals is also available, as well as transport and storage containers. Prototype Kapton cables of various designs are available. A back-up solution with PEN is being worked on. Test facilities for the various components of the detector array are either completed or in commissioning.

4 Front-End Electronics

In the last semester, the activity on the front-end electronic design has been focused on the production and characterization of ASIC CMOS chips in both R&D programs pursued by the collaboration.

XFAB 0.6μm CMOS technology fully integrated preamplifier: the F-CSA104 preamplifier has been designed to be a fully integrated low-noise 4 channel preamplifier. It is shown in Fig. 7. Each chip contains 4 channels of a charge sensitive preamplifier (CSA) followed by a 11.7 MHz line driver. The F-CSA104 chip has been custom designed for GERDA: it is a γ-spectrometry class preamplifier designed to be operated at cryogenic temperatures. The first production run was performed beginning of 2006 and chips were tested during this summer. The tested chips behave as expected in terms of sensitivity and bandwidth apart from the noise figure that is a factor two above specification in the current tests. Tab. 1 summarizes the relevant characteristics of the F-CSA104 chip as measured with the test board (shown in Fig. 8). Fig. 9 shows the noise figure as a function of the input detector capacitance. The minimum ENC (Equivalent Noise Charge) at $C_{det} = 30pf$ is found to be 250 e^- r.m.s.. We are confident that the excess noise compared to the design value (reported in the same figure with the green line) comes from the test board, therefore it can be further improved.

CZX 0.8 μm CMOS technology: Two circuits have been designed and realized using this technology. One (PZCSAv1) where the amplifier is integrated, while the input FET and feedback components are external SMD components, another (RPCSAv1) which is fully integrated. The PZCSAv1, shown in Fig. 10 is a single ended CSA, characterized by an open-loop gain $A > 10^5$A, and stability $< 0.1\%$; it has been produced and tested in years 2005-2006. Results have been already reported to this committee in spring 2006; they fully meet the bandwidth, sensitivity and noise specifications, and are summarized in Tab. 1. The noise figure as a function of C_{det} is shown in Fig. 11. The minimum noise, at 77 K, is 110 e^- r.m.s and occurs at $10\mu s$ shaping time. The circuit can properly drive a 10 m long 50 Ω cable as depicted in Fig. 12)

The fully integrated version has been produced during this summer, it includes a tunable CSA dual power supply with no additional V_{refs}, variable input g_m, R_0, followed by a fully differential line driver. The design full swing of the CSA plus line driver is 2 V on 100 Ω, the power consumption is tunable and the current varies from 3 mA up to 6 mA at full bandwidth. The chips are at presently under test and characterization.

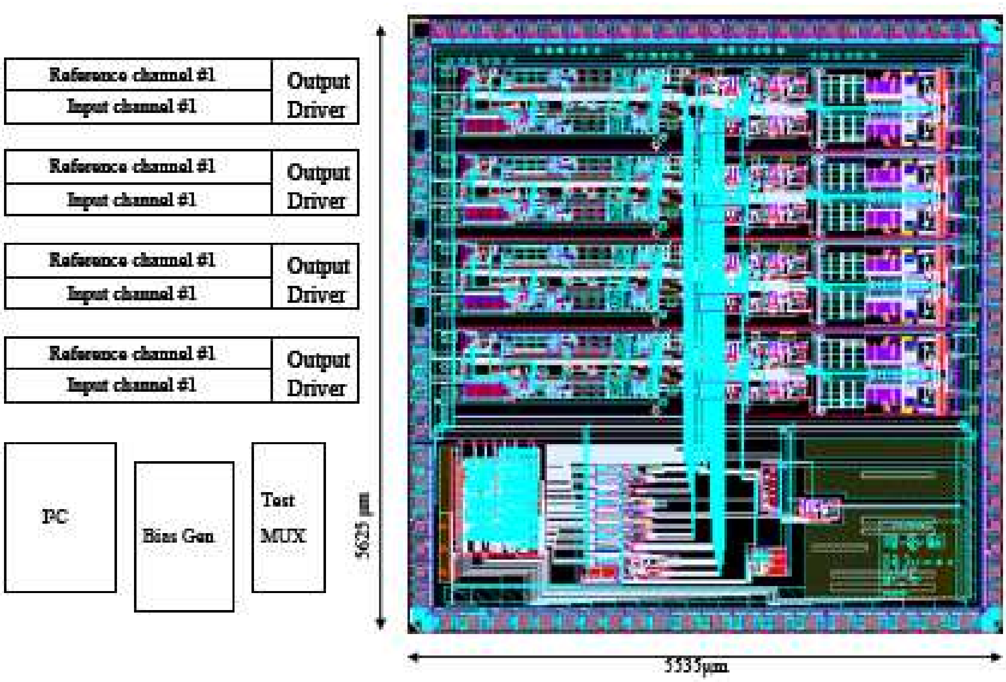

Figure 7: The F-CSA104 4 channel charge sensitive preamplifier.

I(ntegrated)PreA(mplifiers)(v)4: The monolithic JFET semi-integrated CSA has been finalized for the test with detectors. 20 channels have been produced for prototype testing. The preamplifier is mounted on a custom designed Diclad 880 PCB. It is shown in Fig. 13. During August it has been submerged for tests in liquid argon in the LArGe underground facility. At $C_{det} = 0$ the measured noise figure is 0.8 keV, for an input test charge corresponding to 1.332 MeV in germanium. This excellent noise figure confirms the measurements previously performed at the test bench, which are characteristic of the JFET buried layer technology. The power consumption is quite high when compared to CMOS circuits, being $\approx$ 100 mW. This solution is used during prototype tests until the ASIC circuits are available.

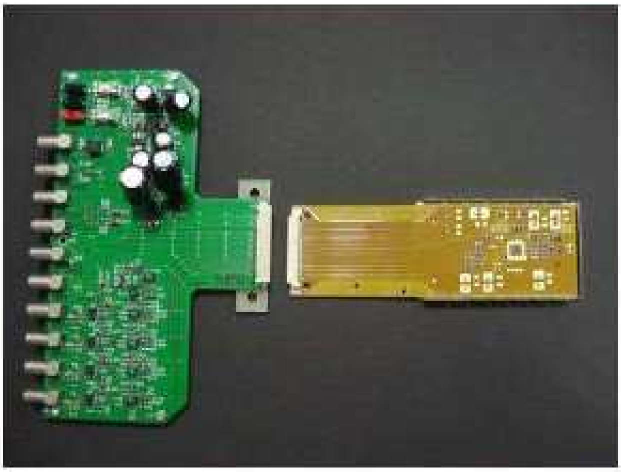

Figure 8: The F-CSA104 4 channel charge sensitive preamplifier mounted on the kapton test board: the shaping amplifier used for the noise measurement is also shown.

	T [K]	Sensitivity [mV/MeV]	rise time [ns]	ENC/shaping time [num. of e^-]/[μs]	power [mW]
F–CSA104^A	300	250	18	280/20	50
	87	250	10	240/20	50
PZCSAv1^B	300	150	15	156/2	-
	77	150	15	180/10	25
IPA4^A	300	130	60	130/10	110
	87	150	50	150/10	110

^{A} Tested with 10 m long cable.
^{B} Tested with short cable

Table 1: Measured characteristics of the three charge sensitive preamplifiers under development for GERDA. ENC values are quoted for $C_{det} \sim 30$ pF

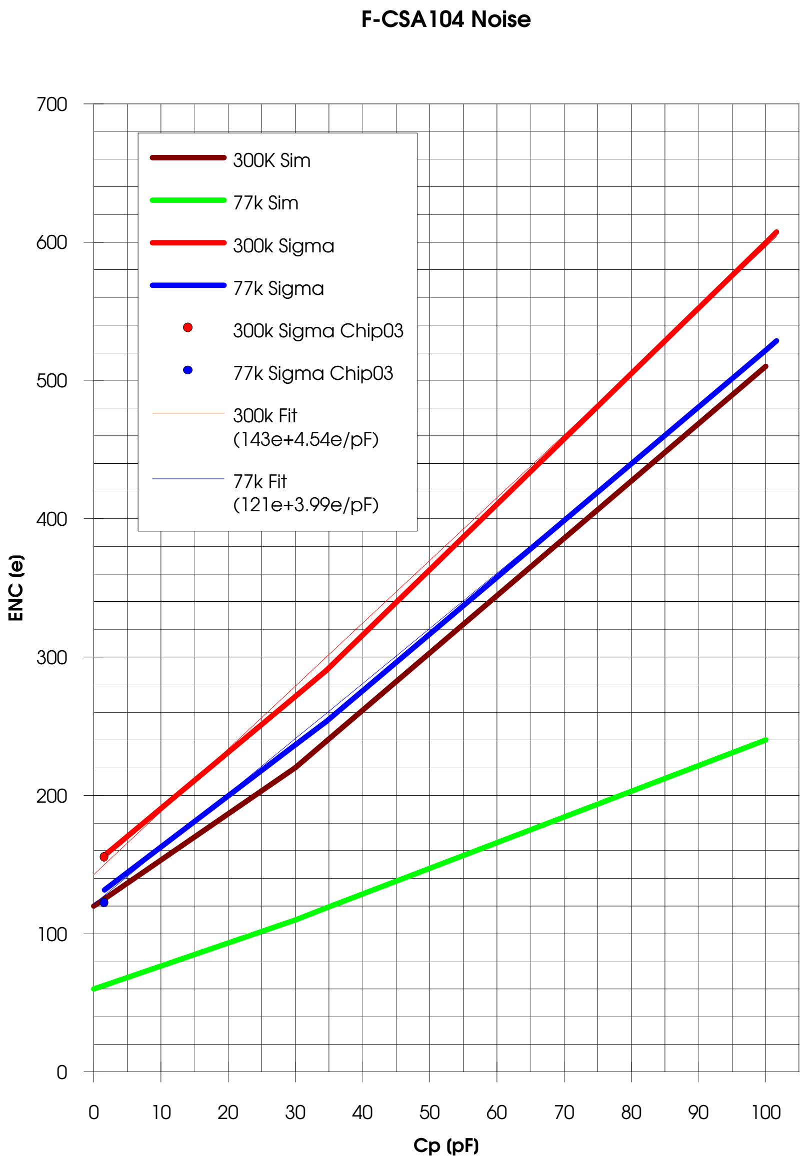

Figure 9: The measured ENC of the F-CSA104 as a function of the detector capacitance. The simulated ENC values are shown for comparison: the lower (green) line corresponds to 77 K and the second lower (brown) line to 300 K.

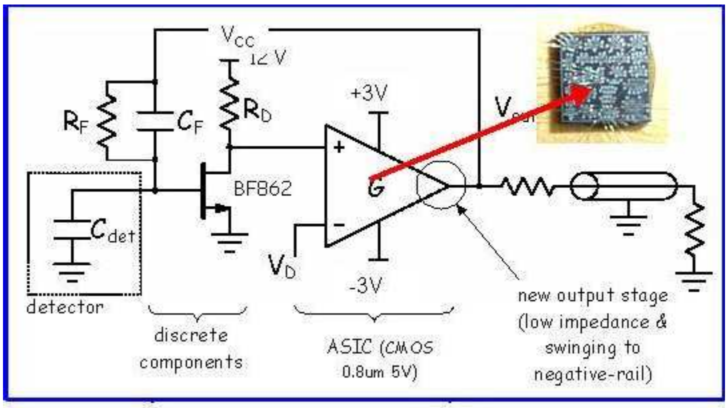

Figure 10: Semi-integrated single ended CSA ASIC, produced in CMOS 0.8 μm technology.

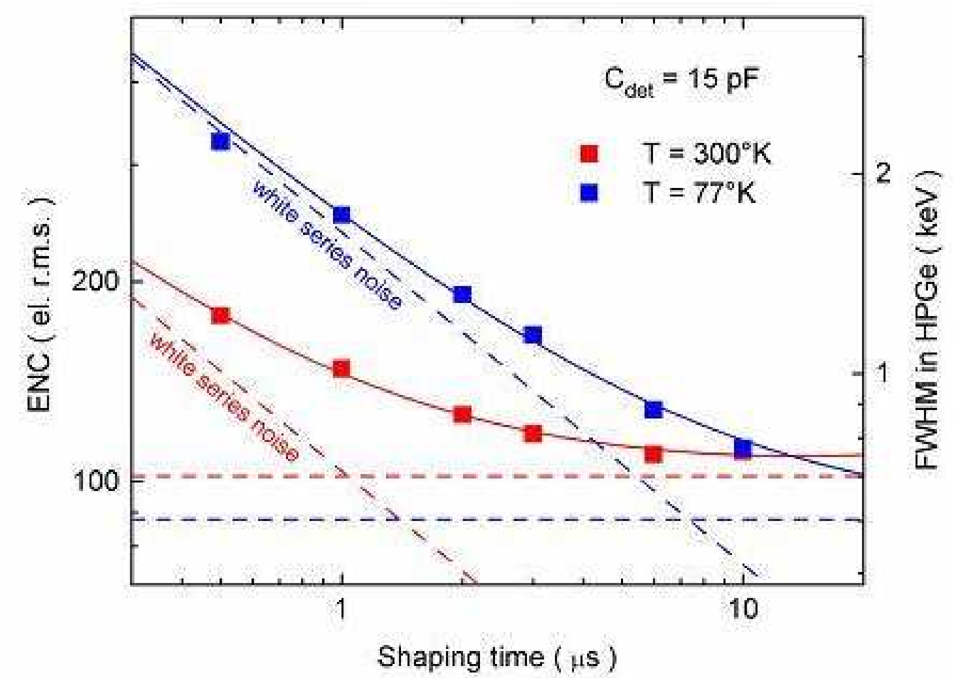

Figure 11: Measured noise figure of the single-ended CZX ASIC CMOS 0.8 μm

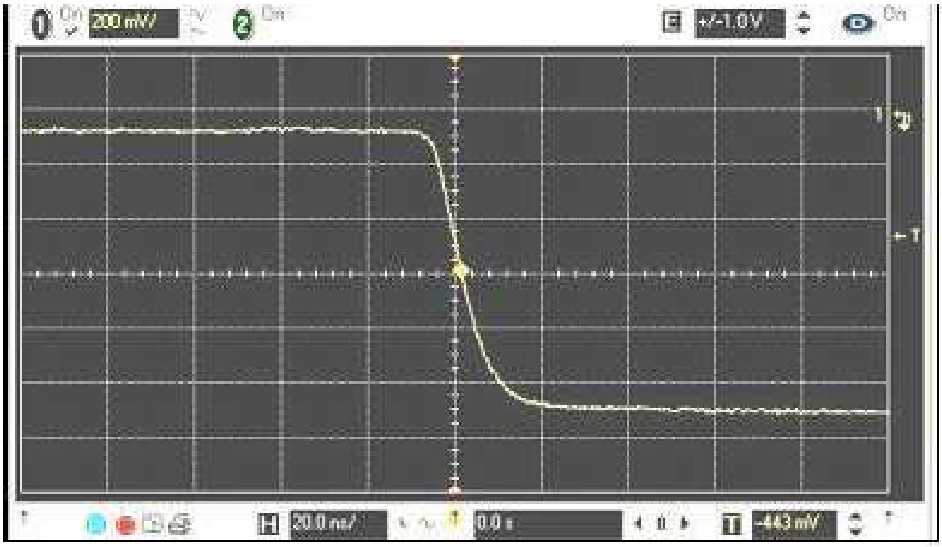

Figure 12: Acquired output signal of a semi-integrated single-ended CZX ASIC, driving 10 m long 50 Ω coaxial cable: the rise time is 15 ns.

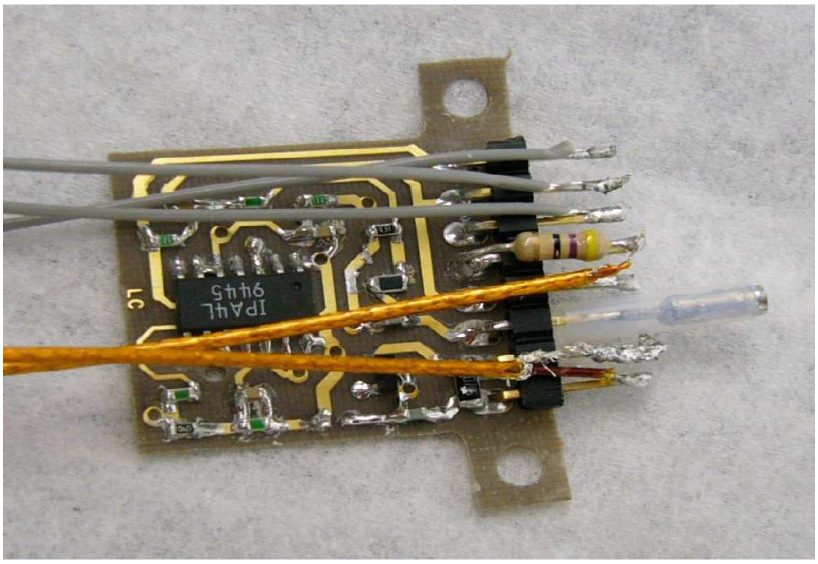

Figure 13: IPA4 CSA mounted on its PCB connected to cables for the LAr test.

5 DAQ Electronics and Software

The INFN Padova in collaboration with INFN Milano has updated their DAQ system for germanium detectors. It uses now 14-bit 100 MHz Flash-ADC chips. The FADCs are mounted on NIM modules (see Figure 14). The effective number of bits of the system was measured to be 11.5 and hence well above our requirement of 10. The daughter board for the analog input stage can be configured for single ended signals with adjustable offset and polarity or differential signals. Thus, this system is very flexible and modular. All possible scenarios for the analog inputs are accomodated.

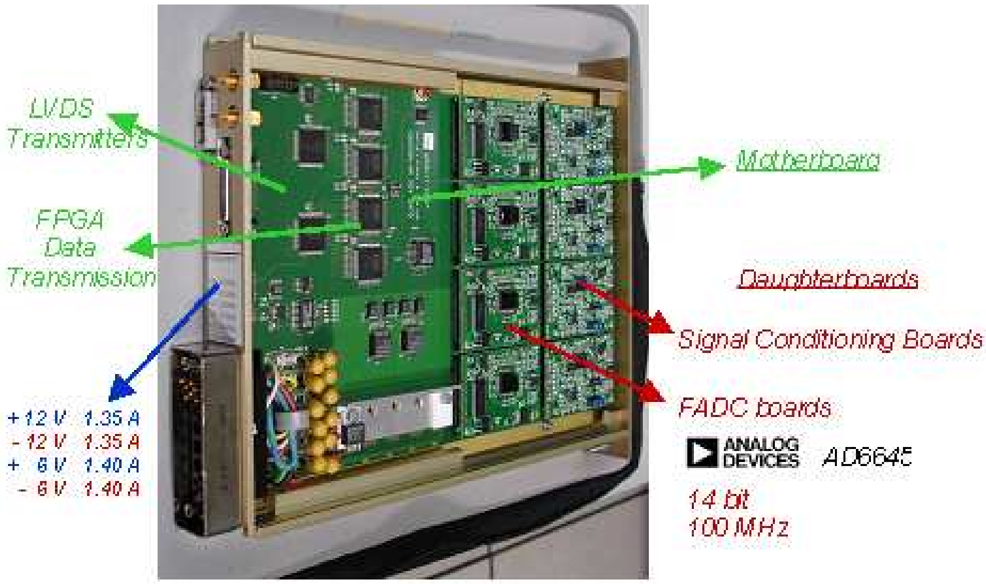

Figure 14: The four channel 100 MHz, 14 bits FADC developed and built for GERDA Phase I.

The FADC data are sent via low voltage differential signals (LVDS) to a CERN built PCI card, where they are stored in memory. The trigger is generated externally from copies of the analog preamplifier signal with standard NIM electronics (Constant Fraction Discriminator, Fan In–Fan Out, Dual Timer, Octal Gate Generator, Coincidence Unit) and also sent to a PCI module which then generates an interrupt for the PC. The CPU reads out the data from the PCI card memories and store them on a 500 GBytes Ethernet hard disk. In addition, this PC acts as a data server such that other clients can access the data for monitoring and analysis purposes.

A system with 8 channels was installed in July at LNGS and 24 channels will be ready by the end of this year.

It includes not only the hardware but also a graphical user interface for the control of the DAQ and JAVA based data analysis and on-line monitoring programs running on the above mentioned clients. Thus, in a few months a complete DAQ system for phase I will be available.

In parallel, 240 FADC channels of the Struck SIS3301 module have been bought already for the readout of segmented detectors.

The slow control system for monitoring of temperatures and pressures as well as for the operation of the high voltage will be developed once the hardware becomes available. This is not considered to be a time critical item.

6 Cryostat and Cryogenic Infrastructure

The baseline design for the GERDA cryostat was a superinsulated double-walled container manufactured almost completely from copper of extremely low radioactivity. To keep the radiopurity of the copper material, electron beam (EB) welding in a vacuum chamber was chosen as welding technique. The design of the system was well advanced, and all TUEV electron beam welding certificates were in hand; moreover, 70t of high purity copper had been ordered. In March 2006, the MPI Heidelberg received from the electron beam welding company 'Pro-Beam' the definitive quote for welding the copper cryostat including the machining of the individual parts and the building of the welding jigs. This quote was a factor three higher than the initial estimates. Moreover, the third wall which had been requested for a copper cryostat created technical difficulties and additional costs.

As to this new situation, the GERDA collaboration agreed in a meeting on March 24 on the following conclusions: (i) The GERDA collaboration as a whole does not have the resources to cope with the additional cost. (ii) Contacts with other suppliers for electron beam or TIG welding should be started. (iii) The backup solution outlined in the Technical Proposal, a double-walled superinsulated stainless steel cryostat with internal copper shielding, should be studied in more detail. Since the contacts with other suppliers did not yield the desired result, the collaboration decided at a meeting on May 29, to go ahead with the backup solution. For appropriate background performance, the stainless steel cryostat requires the use of liquid Argon (LAr) as shielding and cryogenic liquid. Computer simulations of muon induced neutron backgrounds were found to be acceptable for the pursuit of neutrinoless double beta decay. It is clear, however, that less experience exists for this solution and additional uncertainties remain for the background estimates of the neutrons produced in the cryostat. As to the operation of the Ge diodes in LAr, the collaboration has found so far no effects which would indicate the presence of LAr specific problems.

The design of the superinsulated stainless steel cryostat is shown in Fig. 15; Fig. 16 provides a 3D view, and typical features and specifications are listed in Table 2. The design and the specifications [4] are very similar to that of the copper cryostat with its inner container resting on pads of low thermal conductivity in the outer container. The inner vessel is designed according to AD2000 and the European pressure vessel codes for an overpressure of 1.5 bar while the operating pressure is less than 0.5 bar; the outer vessel is designed also according to AD2000 for an outer water pressure of 0.8 bar. The whole system is designed for an earth quake resistance without damage of 0.6 g horizontally and vertically. While the vessel height of 8.9 m is kept and the outer diameter has been changed from 4 to 4.2 m, the height of the cylindrical part has been increased to 4 m corresponding to an increase in volume from 50 to 70 m^3. This increase eliminates the need of an internal copper shield at the top vessel head. The internal copper shield for the cylindrical wall will rest on a steel ring at the bottom of the cylindrical wall; its fixation will use another steel ring at the top of the wall. The thickness of the copper shield has been determined by Monte Carlo simulations and depends of course on the radiopurity of the stainless steel material. For an activity of about 10 mBq(^{228}Th)/kg and LAr filling, typically 40 tons of copper would be needed. With a liquid nitrogen filling (LN_2) the amount of copper would triple implying unacceptable cost.

The tendering process for the cryostat started with a 'Prior Information Notice' [5] in June; the tendering document [6] was published in August. By the deadline of September 29, quotes from 6 companies were received. In view of the shortage of stainless on the world market, a major part of the stainless steel for the cryostat has been ordered already earlier by the MPI. The contract allowed to return material of too high radioactivity. The screening results obtained so far (see section 13) indicate the steel's ^{228}Th activity with less than 2 mBq/kg to be significantly lower than expected. Depending on the quoting company, the production time of the cryostat will be 6 to 9 months.

A 'Process and Instrumentation Diagram' (PID) for the cryogenic infrastructure has been presented already in the September 2005 Progress Report (see Fig. 6 there). Taking advantage of the favourable boiling point of LAr (10 K higher than LN2), the active cooling system could be considerably simplified by passing a controlled LN2 flow from a storage tank through the heat exchanger. The tendering for the cryogenic infrastructure is not time critical and will begin before the end of the year.

LNGS has requested for the new crostat system another safety review which has started with a meeting at Assergi in June. The risk analysis is performed by NIER, Bologna; it is based on the Technical Specification for the cryostat [4], an updated draft of the GERDA Technical Proposal (Version 0.2), and additional ad-hoc written information. A preliminary version of the Risk Analysis [7] was discussed at CERN on September 18 and 19. The design of the GERDA experiment and of the new stainless steel cryostat is accepted. The consequences of a leak in the inner or outer container will be mitigated by the implementation of (i) a hermetic plastic skin on the outer surface of the outer container, and (ii) a thermal insulation limiting the heat flux in the cylindrical part of the cryostat to less than 5 kW/m^2. The clarification or optimization of a few other details is still in progress. The final safety report for GERDA by the LNGS safety department is expected to be available for this session of the Scientific Committee.

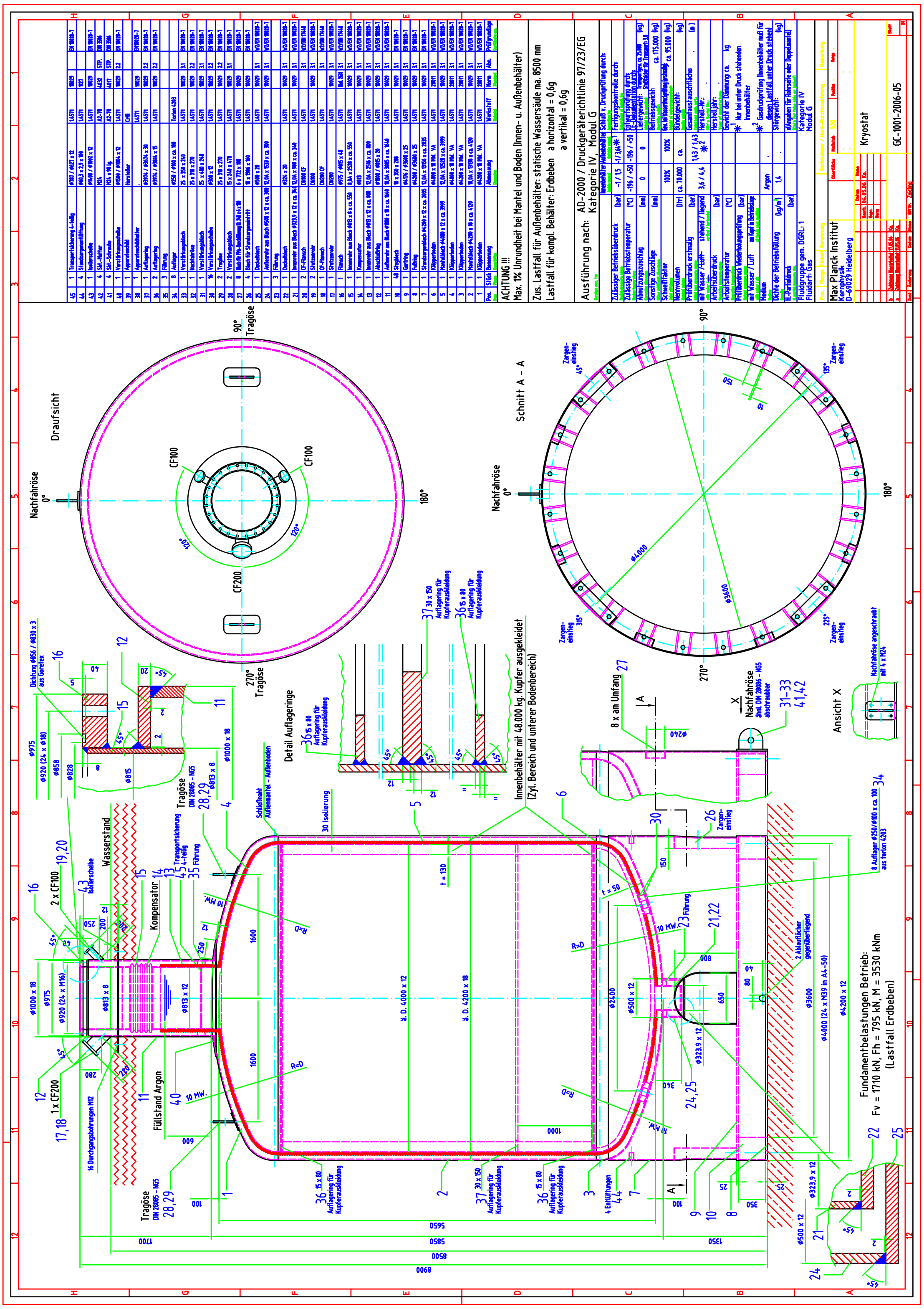

Figure 15: Technical drawing for the GERDA stainless steel cryostat.

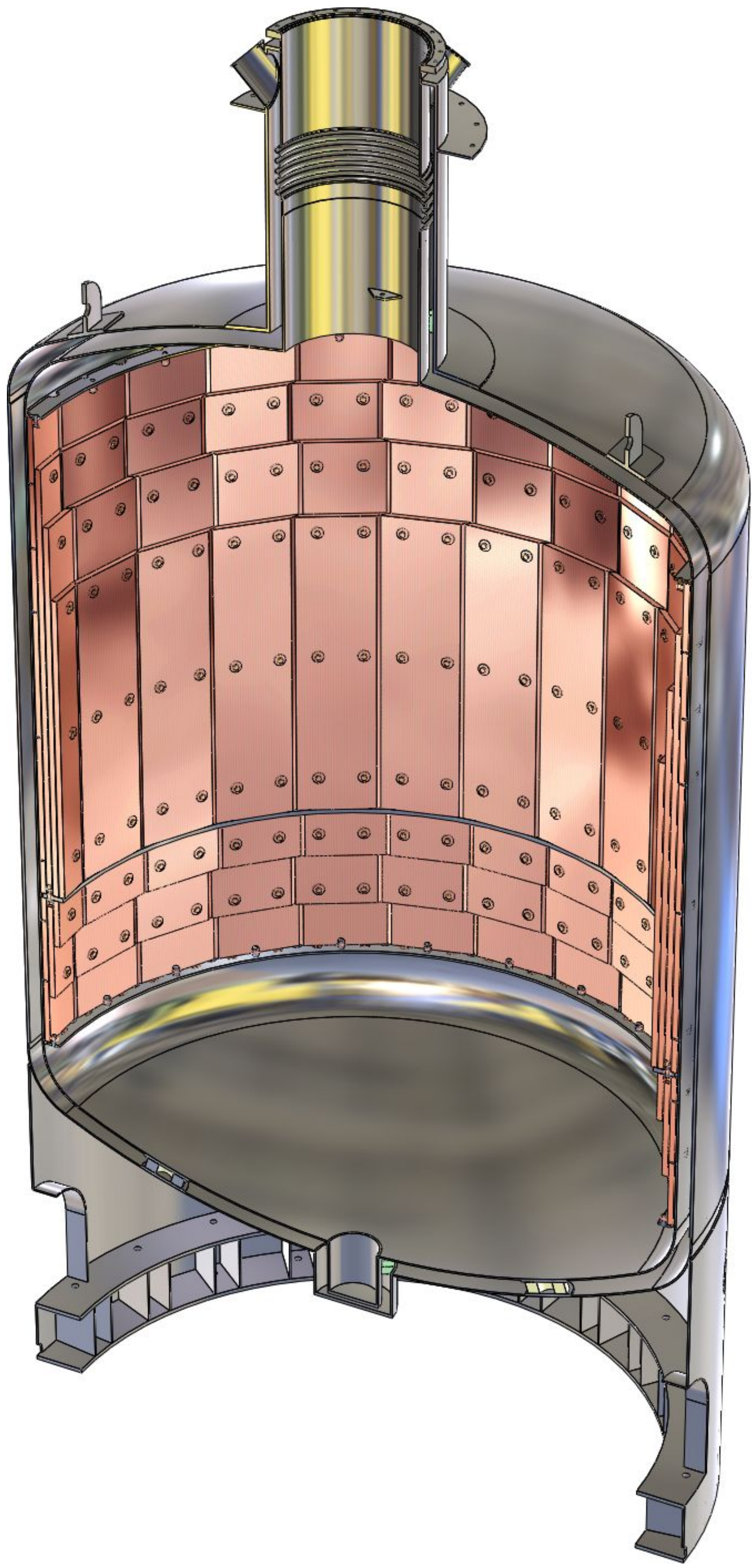

Figure 16: Artist's view of the superinsulated stainless steel cryostat with internal copper shield

Table 2: Characteristics of the GERDA stainless steel cryostat. Please note that for the cylindrical vessel shells a lower radioactivity, <5 mBq(^{228}Th)/kg, is aimed at.

Construction Code	AD2000 HP DGRL 97/23 EG	
Materials and Radiopurity		
vessel	1.4571	<10 mBq(^{228}Th)/kg
compensator	dto.	
multilayer insulation (MLI)	alum. polyester	$<$ 2$\times$ steel activity
pads	Torlon	<5 mBq(^{228}Th)/kg
Cu shield	OFRP copper	$<$ 20 μBq(^{228}Th)/kg
Geometry		
overall dimensions $\varnothing_{outer}\times$height	4200$\times$8900	[mm$\times$mm]
neck height	1700	[mm]
neck inner diameter $\varnothing_i$	800	[mm]
top flange at neck	($\varnothing$975$\times$40)	[mm]
inner vessel volume	$\approx$ 70	[m^3]
LAr fill level	6350	[mm]
Masses		
empty vessel	$\approx$ 25,000	[kg]
max. load inner vessel		[kg]
LAr	$\approx$ 98,000	[kg]
Cu shield	$\leq$ 48,000	[kg]
total mass	$\leq$ 175,000	[kg]
Pressures (w.r.t. atm. pressure)		
inner vessel operating pressure	$<$ 0.5	[10^5 Pa]
inner vessel maximum pressure	1.5/-1.	[10^5 Pa]
outer vessel pressure	2.5/-1.8	[10^5 Pa]
pressure for LAr emptying	1.2	[10^5 Pa]
Loads		
top of neck	1500	[kg]
top inner vessel head at r=1 m	3000	[kg]
buoyancy outer vessel	$\approx$ 700	[kN]
Multilayer Insulation		
nominal insulation vacuum	10^{-3}	[Pa]
thermal loss	$\leq$300	[W]
corresponding daily loss of LAr (0.2%)	140	[ℓ]
Special Requirements		
fraction of x-rayed welds	100%	
earthquake tolerance	h/v 0.6 g	
shock tolerance during transport	3 g	
lifetime	10 yrs	

7 Water Tank

The GERDA site in hall A has been prepared to receive the GERDA installations. In particular the water tank (WT) and superstructure foundations and the pipe to drain the water have been put in place. The WT tender closed in March 2006, the winning company has been awarded, and the contract signed. The executive project is in preparation. The WT mounting schedule is strictly interconnected with the cryostat schedule. Both the mounting procedure and schedule are in preparation: it is planned to build the bottom plate and then put the cryostat in place and perform the cryostat test plan, before the completion of the WT construction.

8 Muon Detector

In order to suppress the expected direct background from external muons at LNGS (3600 mwe.) from $2 \cdot 10^{-3}(\mathrm{keV} \cdot \mathrm{kg} \cdot \mathrm{y})^{-1}$ to a level well below the GERDA design background rate of $10^{-3}(\mathrm{keV} \cdot \mathrm{kg} \cdot \mathrm{y})^{-1}$, the installation of an external muon veto is necessary. A water Cherenkov detector will be installed in the outer water shielding volume, contained in a 630 m^3 steel tank. 60 photomultipliers (PMTs) will be fixed to the tank, and other six PMTs will especially look on a small water volume (pillbox) directly below the liquid argon cryostat. Concerning fixation and installation of PMTs and cables, most technical items have been worked out. The positions of the PMTs have been determined by computer simulations predicting a muon veto efficiency above 95%. Every photomultiplier will be encapsulated by a water-tight stainless steel housing with a polyethylene window; this design corresponds with slight modifications to the design developed for the muon veto of the solar neutrino experiment Borexino and is successfully working in the Counting Test Facility since five years. New tests with PMTs encapsulated are under preparation at Tübingen University. A water-tight cable connects high voltage and signal from each PMT separately to the data acquisition set-up outside the tank. A 'cable chimney' providing air-tight feed-through for the PMT cables to the roof of the tank has been designed. All surfaces around the active water volume of the muon detector will be covered by a reflector foil (VM2000) to increase the light efficiency of the detector. The main components, i.e. steel, PMT glass and reflector foil, have successfully passed the the radio assay with germanium spectrometry. Additionally, plastic scintillator panels above the tank compensate for missing active water volume around the cryostat neck.

9 Main Experimental Site

The main experimental site of the GERDA experiment is located in hall A, in between the TIR tunnel and the LVD experiment. Precision surveys have been performed using laser techniques. The result of these measurements have been used to determine the spatial limits which have to be respected by GERDA. These limits are indicated in Fig. 18, 19 and 20.

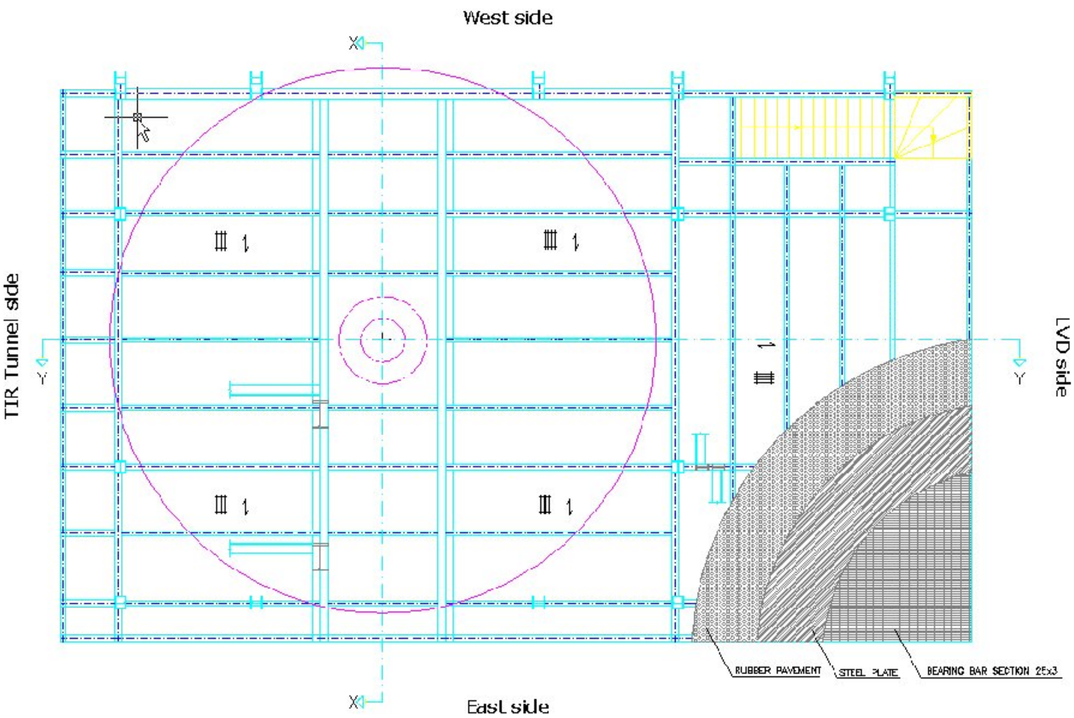

Figure 17: Layout of the top level of the Gerda building. The clean room and the lock will be placed on top of this platform by TG5.

The Gerda area has been refurbished in the framework of the commissioner's activities in order to improve its water tightness, and the connections to the new LNGS water collection system has been prepared. In this context also the anchorage points for the Gerda Building and the Gerda WT have been finalized. The work has been completed during summer 2006 and the site is now ready to host Gerda.

10 Gerda Building

The design of the Gerda Building has been finalized (see Fig. 17, 18, 19 and 20). The preparation of the executive drawings performed in close collaboration with TG4 (cryogenic vessel), TG5 (Infrastructure on top of vessel) and TG6 (Water Vessel) will be concluded by October 10. The weight of the lock (15 t) and of the clean room are taken into account. The motion of the system as a whole in case of earthquake will be analysed. Also the constraints arising from the coupling of the cryostat with the lock, which is connected to the Gerda Building are being considered.

LNGS has received an extra 260 kEuro from the Executive Board of INFN. This money is sufficient for setting up the shell of the building while additional money is needed for the general plants like electrical equipment and basic safety system. The tendering process of the shell of the building will start by November. The construction of the building can

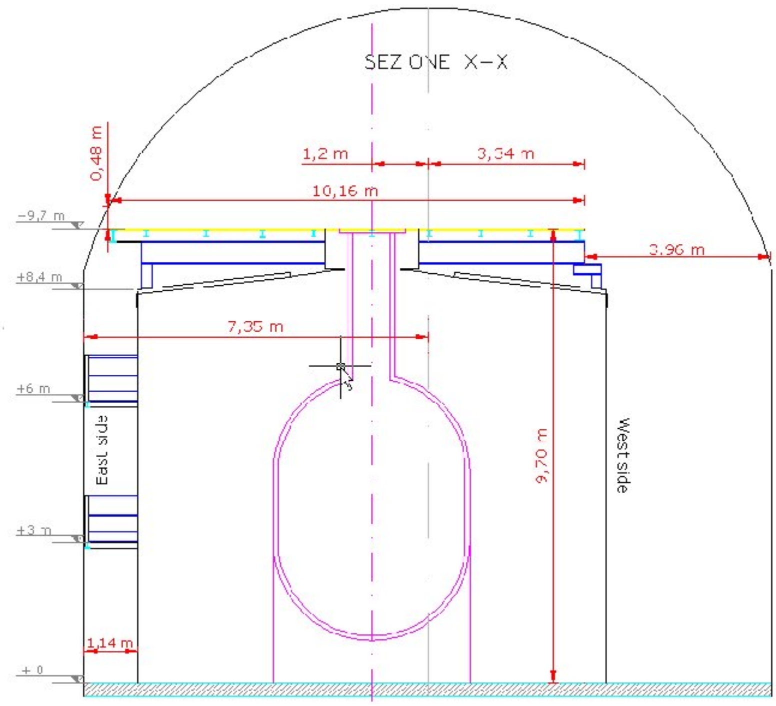

Figure 18: Section (view from LVD) of the GERDA building together with the constraints given by the installations present in Hall A.

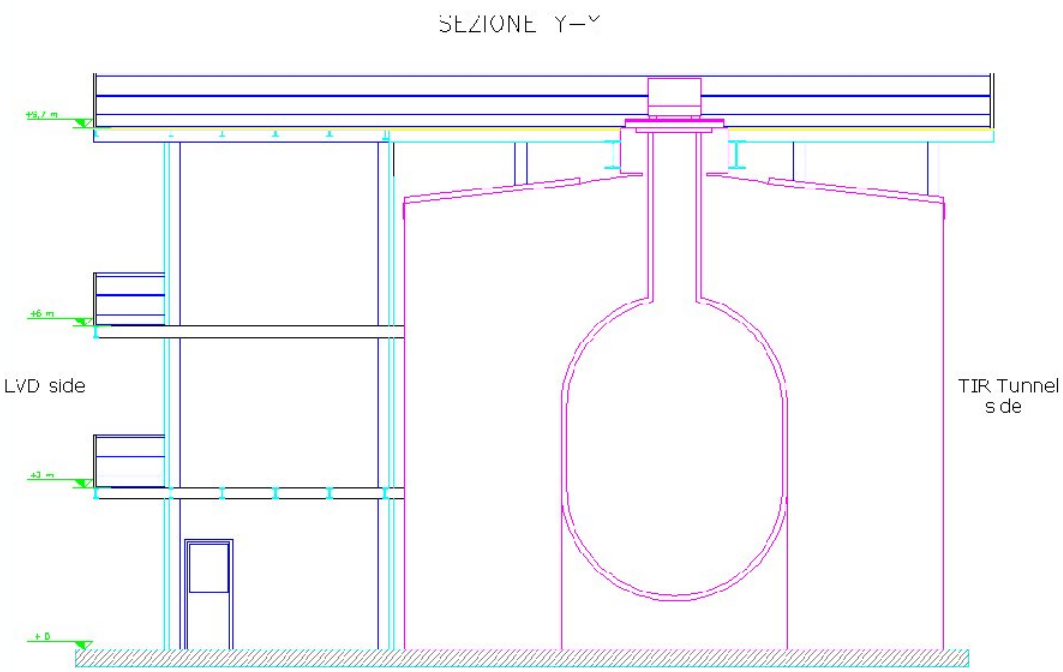

Figure 19: Section (side view) of the GERDA Building.

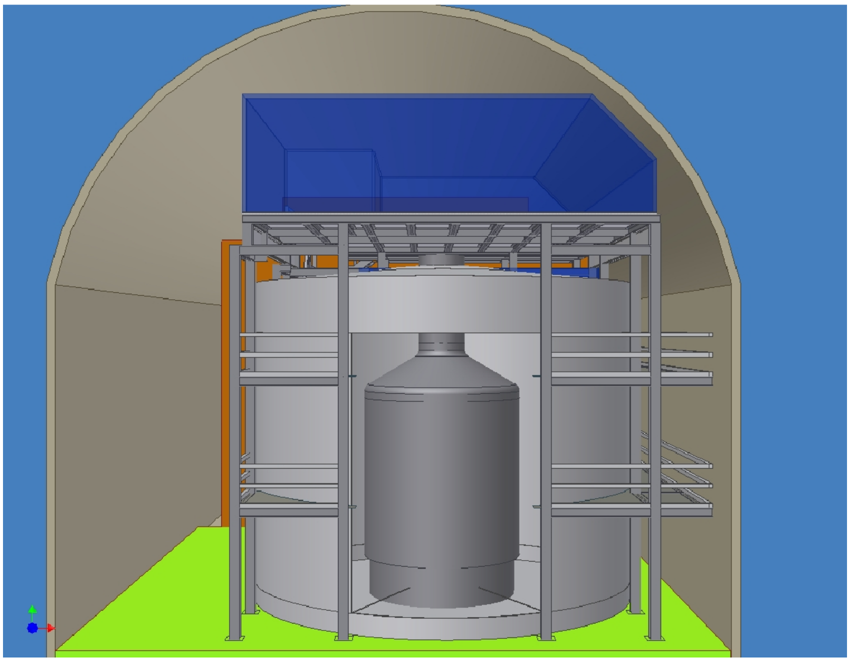

Figure 20: View of the GERDA experiment in hall A. The constraints arising from installations in hall A are included. The cryostat and clean room on the platform of the GERDA building are shown.

start in June 2007.

11 Infrastructure on Top of the Platform

The clean room located on the platform of the GERDA building is ready for tendering, pending the final confirmation of available space. The operational parameters are defined and the infrastructural requests to LNGS were made. The class 10000 clean room will have radon–reduced air and will be constructed from stainless steel (see fig. 21).

Solutions for all technical issues regarding the lock and the internal loading systems are available. A number of materials were found to be acceptable by task group 11 with respect to radon emanation and, if relevant, gamma emission. More tests are pending. The detailing of the various components is under way as well as the development of a construction sequence. Fig. 22 shows the design of the lock system composed of inner and outer lock. Magnetic arms allow mechanical transfers in the inner lock. The cables permanently installed in the lock systems are pulled up into the two arms of the inner lock.

The rail system which guides the strings to their final position and from which they are lowered is currently prototyped at the MPI Munich. It is depicted in Fig. 23. Visible are the moving sleds which provide the interface between the permanently installed cables and the cables of the string. One detector string in the process of being lowered is shown. It is planned to completely assemble the lock and the loading system at the MPI Munich

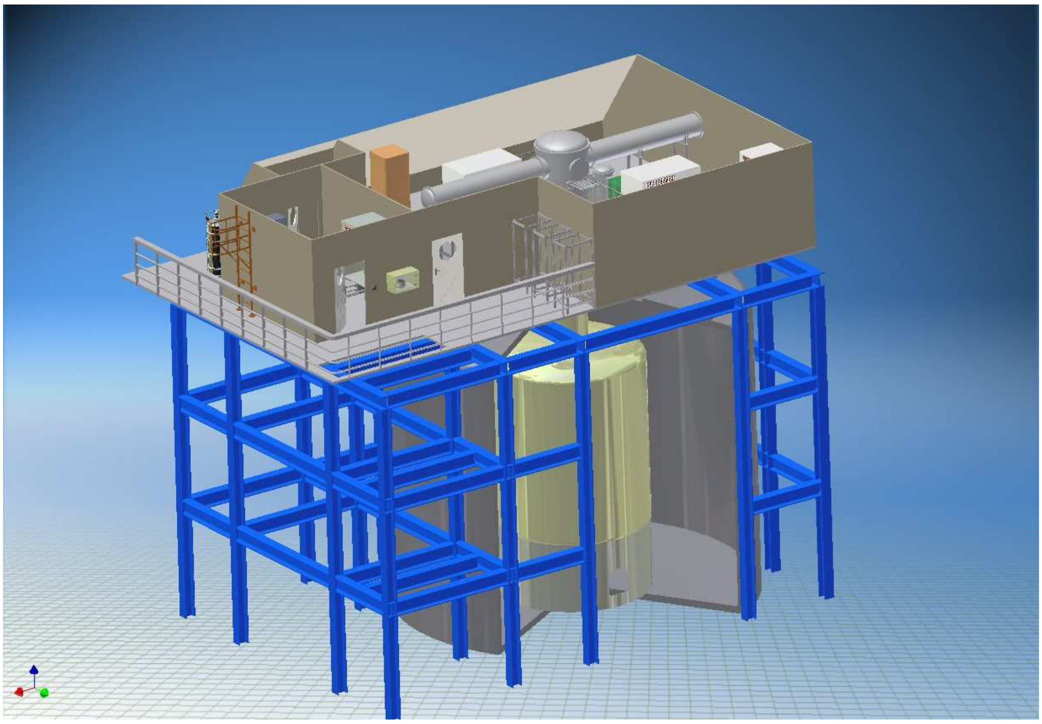

Figure 21: The clean room is constructed on the platform. It is accessed through a personnel lock and contains the lock system and the supporting infrastructure.

before shipping the parts to LNGS.

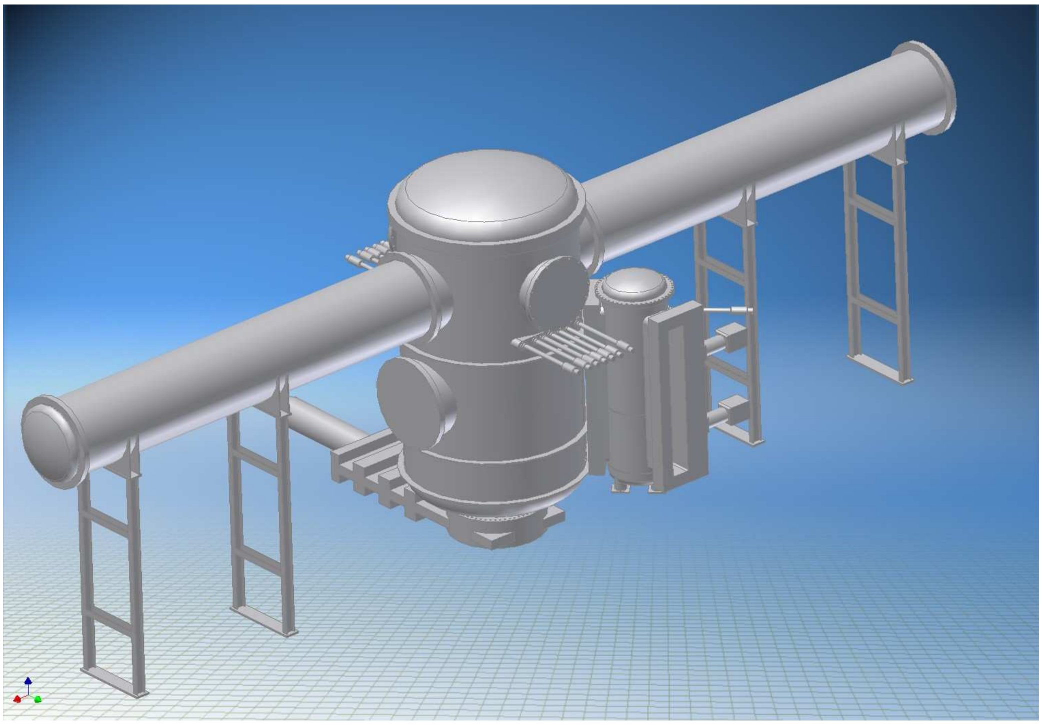

Figure 22: The lock system with the inner and outer lock. The system is connected to the neck of the cryostat with a vacuum shutter followed by a bellow and manifold.

Figure 23: The rail system to position and lower individual strings.

12 Monte Carlo Simulations

The Monte Carlo group task group (1) simulates the GERDA setup and estimate possible background contributions, (2) supports other task groups in the design of detector components for GERDA and (3) supports R&D projects by simulating individual setups.

The MaGe framework, developed in close cooperation with the Majorana collaboration, is the basic tool to fulfill these tasks. It is a Monte Carlo tool based on the GEANT4 framework. Further details and applications of MaGe can be found in [8, 9, 10]. Recent projects are presented in the following.

12.1 Muons

A simulation of cosmic muons has been performed in order to guide the arrangement of photomultipliers (PMTs) inside the water tank. This Cherenkov detector is an integral part of the GERDA muon veto and has been optimized by extensive Monte Carlo studies using the angular distribution of muons measured at LNGS as depicted in Fig. 24 (top, left). The optimized setup consists of 40 PMTs on the wall and 20 PMTs on the bottom of the water tank. Additional 6 PMTs are mounted onto the skirt below the cryostat facing inwards.
Studies of muon induced photon and neutron production were performed for the GERDA setup [9]. Both, the prompt and delayed background contribution were estimated and found to be reducible to the desired level using the muon veto system. These studies were also used in the decision to change the baseline design to a steel cryostat.

12.2 Detector segmentation and design studies

Detectors deployed in the second phase of GERDA will be segmented. Studies of different segmentation schemes have been performed with respect to the background reduction power and signal efficiency. Fig. 24 (bottom) shows the suppression of events from two particular background sources for different segmentation schemes. Both, liquid nitrogen and liquid argon haven been used as cooling medium. An estimate on the background reduction using 18-fold segmented detector can be found in [10]. The possible additional background from electronics and cabling was also evaluated.

This guided a redesign of detector components such as the suspension system and readout cables. Background contributions from each component are estimated and limits on the radio-purity of materials are given. The limits can be compared with results from material screening and thus the complete design can be evaluated.

Alternative designs for the detectors are also studied, e.g. small and unsegmented diodes. These studies focus on the background reduction and achievable sensitivity.

12.3 Monte Carlo verification

Test stands for detector development are accompanied by Monte Carlo simulations. The deviation of data and Monte Carlo is of the order of 5-10%. Fig. 24 (top, right) shows a ^{60}Co energy spectrum for a 18-fold segmented detector measured with the core electrode compared to Monte Carlo plus background data. The good agreement justifies the use of the Monte Carlo in the design of GERDA.

Simulations of the LArGe setup using Phase I detectors are also performed and will provide additional verification of the Monte Carlo.

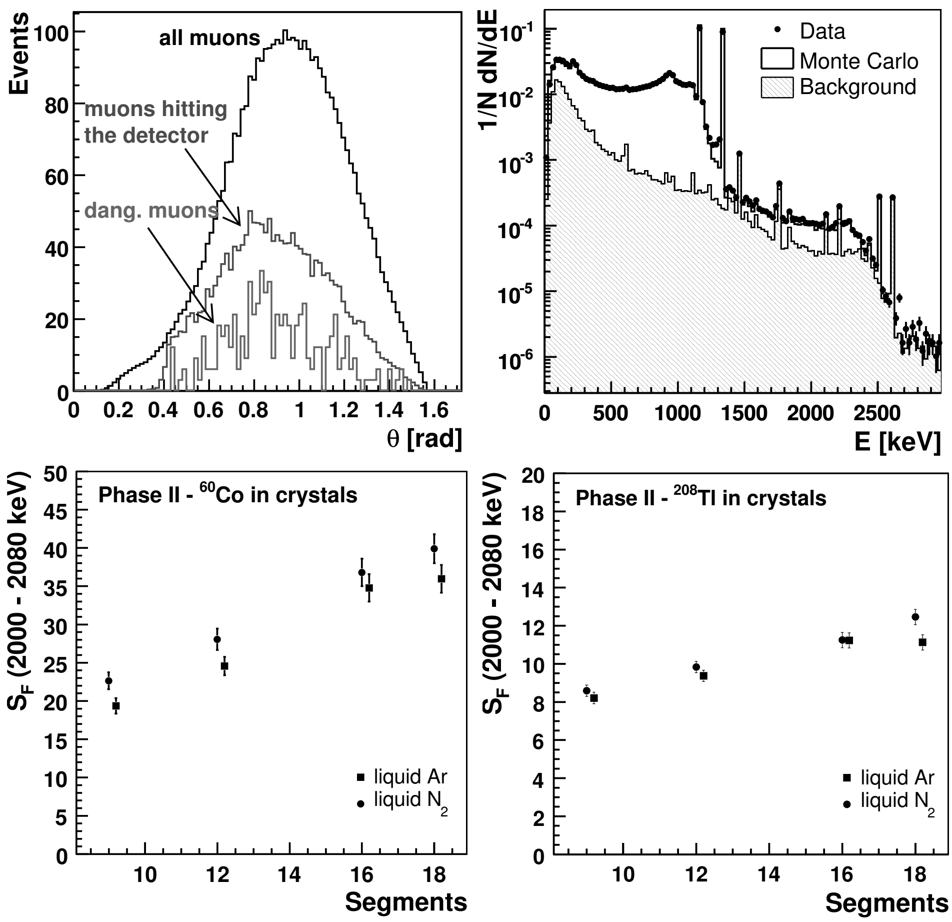

Figure 24: Top, left: Angular distribution of simulated muons. Top, right: Energy spectrum taken with an 18-fold segmented prototype detector compared to Monte Carlo plus background data. Bottom: Suppression factors in the region of interest for ^{60}Co (left) and ^{208}Tl (right) in the crystals.

13 Material Screening

Screening for Gerda construction materials has been continued in the reporting period. This includes γ ray screening, ICPMS measurements, Rn emanation measurements and some further developments and improvements for procedures and instruments applied in these studies.

13.1 γ ray screening

A variety of samples has been measured for radiopurity in the period under review. These measurements have been performed in the low-level laboratories of four Gerdagroups (MPIK Heidelberg, IRMM Geel, INR Baksan and LNGS Assergi). After the decision to construct the GERDA cryostat from stainless steel, special attention has been paid to γ ray screening measurements of stainless steel samples. Results on the relevant radioisotope activities in these samples are presented in Table 3 together with the results for a reflector foil (VM2000 foil, to be used as reflection material on the outside of the cryostat) and for Teflon (used for the Ge crystal holders).

Sample	**Specific activity [mBq/kg]**				
	^{228}**Th**	^{228}**Ra**	^{226}**Ra**	^{40}**K**	^{60}**Co**
SS 1.4571 #495243	< 0.20	< 2.6	< 1.3	< 2.8	45.5±2.1
SS 1.4571 #495257	< 0.59	< 1.9	< 0.89	< 1.7	14.5±0.8
SS 1.4571 #495466-2	5.1±1.0	< 2.9	2.9±1.0	< 3.9	6.5±0.5
SS 1.4571 #494257	< 1.9	< 3.4	< 2.0	< 4.5	14.2±0.6
AISI321 (Outokumpu)	< 1.4	< 0.8	< 1.0	< 4.5	3.8±0.3
SS 1.4541 (Outokumpu)	< 1.1	< 1.4	< 0.8	< 3.3	9.2±0.3
SS 1.4571 (Outokumpu)	3.1±0.3	1.1±0.5	1.2±0.3	< 1.0	15.5±0.6
VM 2000 reflector foil	< 9.0	< 5.7	< 7.9	< 28	–
Extruded Teflon	0.023±0.015	< 0.048	0.021±0.009	0.54±0.11	–

Table 3: γ ray screening results for selected samples.

It turns out that for the actual cryostat design the measured values and upper limits are in all cases below the values required for a background index of 10^{-4} counts/kg·keV·year. Especially important in this context are the first measurements on samples from four (#495243, #495257, #495466-2 and #494257) out of the 8 batches of the 30 t of stainless steel which actually will be used for the cryostat construction.

The four groups performing γ ray screening measurements in Gerdahave participated in an Environmental Radioactivity Comparison study of the National Physics Laboratory (UK). Such a study allows to compare the accuracy of the measurement and evaluation techniques applied by the different low-level counting labs. Discrepancies up to 20% have been observed in some cases, which probably result mainly from errors in the counting efficiency determination for extended samples by MC calculations. While discrepancies on this level are in principle not relevant for material screening in GERDA, some further investigations are under way in order to resolve these inconsistencies.

The increased demand for γ ray screening measurements for GERDAled to the set-up of two new germanium detectors. The first one of 0.93 kg is installed in the Low-Level Lab (LLL) of the MPIK. The sample chamber in the new shield is continuously flushed with nitrogen, resulting in a reduction and better control of the background caused by ^{222}Rn decays in the sample chamber. The second one is a GeMPI-type new detector system which presently is build up in the Ge spectrometer lab at LNGS. All components of the system are available. Currently, the detector shielding parts are cleaned. There is hope that this new detector system will be available for γ ray screening at the beginning of next year.

13.2 ICPMS measurements

An extensive study on the U, Th and K contents of some polymeric substrates by means of an Inductively Coupled Plasma Mass Spectrometer (Agilent 7500a ICPMS) has been performed for GERDAby the LNGS chemistry group. This study included all procedures in cleaning and preparation of the samples for ICPMS. The samples consisted of PET (Polyethylene Terephthalate) and PEN (Polyethylene Naphthalate) with and without metallic cladding. In addition, three samples of super-insulation materials (Coolcat 2, NAC-2, Aluminized Teflon) have been measured.

It turned out that the PEN samples are significantly cleaner in U and Th (about two orders of magnitude) than the PET ones. The PEN specific activities for ^{232}Th and ^{238}U (assuming radioactive equilibrium in the chains, to be checked by γ ray screening) are compatible with the required purity of the cables surrounding the Ge crystals. Two of the superinsulation materials (Coolcat 2, Aluminized Teflon) are cleaner than the third one, their specific ^{232}Th activity is well (a factor of five) below the required limit.

13.3 ^{222}Rn emanation measurements

The total ^{222}Rn emanation of all materials inside the GERDAcryostat should not exceed 10 mBq. This ensures that the contribution of these materials to the total background index is much less than 10^{-4} counts/kg·keV·year. In order to verify this, ^{222}Rn emanation measurements on Iglidur rolls and a tooth belt which will be part of the system installed in the air lock over the cryostat have been performed. In addition, the VM2000 reflector foil and a copper foil have been analyzed. The copper foil is used to investigate the cleaning of copper surfaces with distilled water. Table 4 summarizes the results. Already simple rinsing with distilled water might be able to remove Rn emanating impurities from the copper surface.

Recently, also the system of the emanation chambers has been upgraded. Upcoming emanation measurements include copper wool, some plastic materials and Ge crystal transportation containers.

Sample	^{222}Rn emanation rate
Iglidur rolls	(13.5 ± 1.9) μBq/piece
Tooth belt	$(175 \pm 11)\mu$Bq/m
VM2000 foil	< 50 μBq/m^2
Cu foil	(1.7 ± 0.2) μBq/m^2 (a) (1.2 ± 0.2) μBq/m^2 (b)

Table 4: ^{222}Rn emanation rates for different samples. The Cu foil was measured twice: (a) before treatment, (b) after cleaning with distilled water

13.4 Radon monitoring

The ^{222}Rn concentration in the air of the clean areas within the GERDAdetector set-up has to be monitored continuously. A well known method which is able to fulfill this task at the required low level is the electrostatic collection of the ionized ^{222}Rn daughter atoms onto a detector where the α decays of ^{214}Po and ^{218}Po are measured. Such a detector was successfully realized for the BOREXINO experiment. For GERDA a redesigned version with an active volume of about 700 l and an applied high voltage of around 50 kV has been set up. It is currently tested at the MPIK. There is hope to reduce the detection limit with this device to a Rn level of less than 100 μBq/m^3.

In cases where sensitivities in the range of Bq/m^3 are sufficient, Lucas cells with ZnS as scintillator and volumes of the order of a liter are used for Rn monitoring. In order to improve the performance of such cells, a prototype was designed and built in which the VM2000 reflector foil is applied as scintillator. This foil has a rather low ^{222}Rn emanation rate (see Table 4). While the background of the prototype came out to be similar to the standard Lucas cells, the efficiency for Radon events is still much lower and therefore must be improved, for instance by coating the VM 2000 foil with fluors.

14 Time Schedule

A new time schedule has been compiled after the LNGS safety review at CERN September 18 and 19, and after receiving the bids for the cryostat tender September 29. The sequence of construction of water tank, cryostat and GERDA Building with platform is now defined. Given the nested design of GERDA, the installation will proceed sequentially. Projects on the critical path are the cryostat, the completion of the water tank after cryostat erection and testing, the GERDA-platform, the lock and and clean room.

The concrete basement of the main GERDA site has been completed during summer this year. The next major step will be the mounting of the water tank base plate. Subsequently, the cryogenic vessel will arrive underground. After completion of a series of tests including leak tests and evaporation rate measurements, the water tank construction will be completed. The construction of the GERDA building with the platform supporting the clean room and lock will follow. Orders have been placed for the water tank and tenders have been closed for the cryostat. The tender for the GERDA building will be published in November. The tender for the clean room is ready and will be opened timely in spring 2007.

The current analysis is based on the contract specifications of the water tank, on the schedules received in the bids for the cryostat, on the specifications given in the GERDA Building tender, and on the schedules of the various other sub-projects as e.g. lock, clean room and cryogenic infrastructure. Fig. 25 summarizes the estimated time required to complete the installations in Hall A. From this analysis, we estimate that germanium detectors can be commissioned in this system by summer 2008. No major contingencies are included.

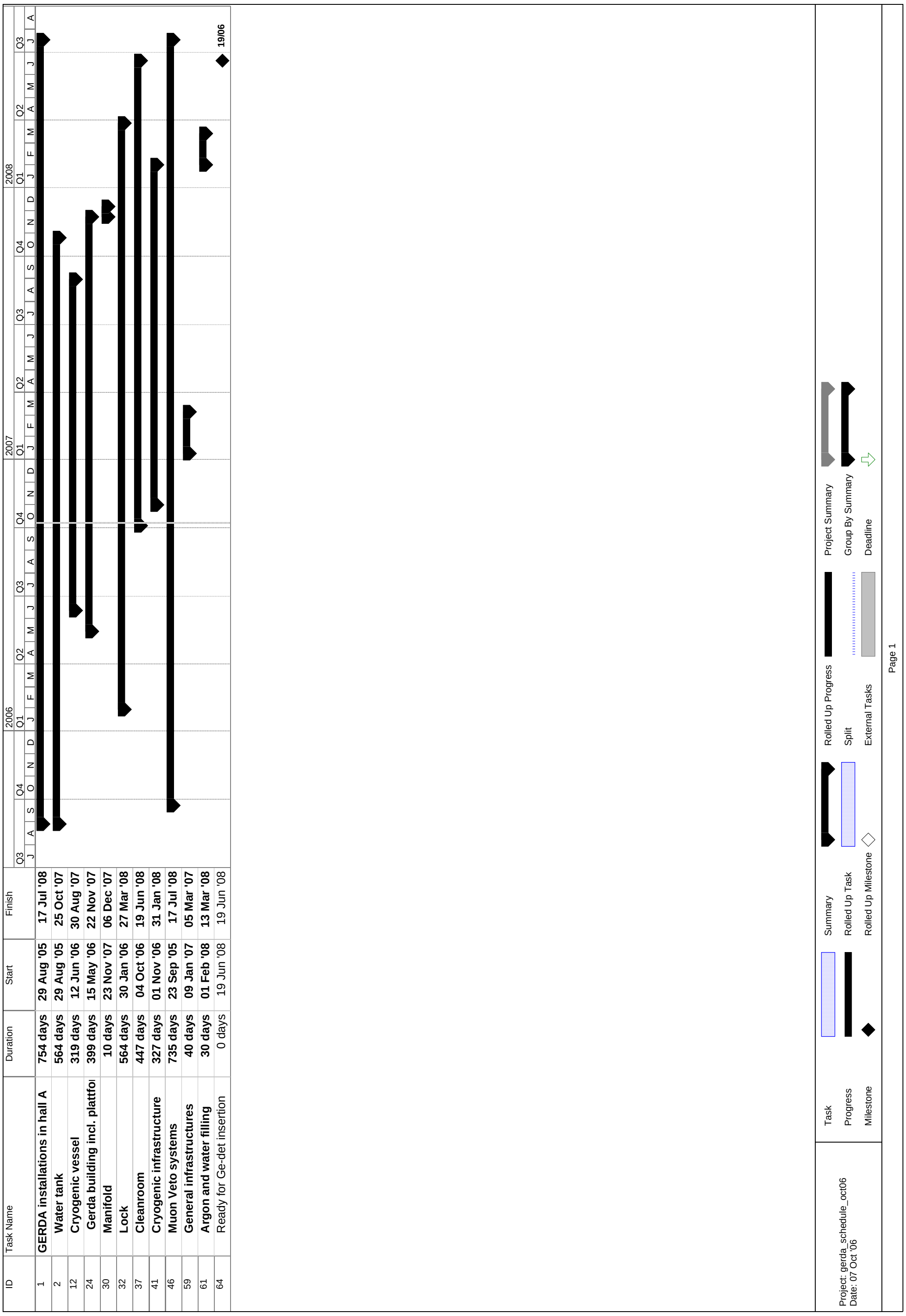

Figure 25: Time schedule for GERDA installations in hall A

References

[1] A. Pullia et al., IEEE Trans. Nucl. Scien. 49 (2002) 5.

[2] P.F. Manfredi et al., NIM A380 (1996) 308-311.

[3] www.amptek.com/a250.html

[4] Technical Specification, Cryogenic Vessel, MPIK, August 8, 2006

[5] Prior Information Notice, TED-publication 113359-2006 (7.6.2006)

[6] TED-publication 164333-2006 (11.8.2006)

[7] Cryogenic and Water Tank System, Risk Analysis, Technical Analysis Phase 1 and Phase 2, Nier Ingegneria S.p.A. for the GERDA Collaboration

[8] M. Bauer *et al.*, Journal of Physics, Conf. Series. **39** (2006) 362.

[9] L. Pandola *et al.* [GERDA Collaboration], accepted for publication in Nucl. Instr. and Meth. A. pre-print LNGS/EXP-05/06, July 2006

[10] I. Abt *et al.* [GERDA Collaboration], submitted to Nucl. Instr. and Meth. A.